Peroxisomal Malate Dehydrogenase Is Not Essential for Photorespiration in Arabidopsis But Its Absence Causes an Increase in the Stoichiometry of Photorespiratory CO_2 Release[1][W][OA]

Asaph B. Cousins*, Itsara Pracharoenwattana, Wenxu Zhou, Steven M. Smith, and Murray R. Badger

School of Biological Sciences, Washington State University, Pullman, Washington 99164–4236 (A.B.C.); Australian Research Council Centre of Excellence in Plant Energy Biology, Molecular Plant Physiology Group, Research School of Biological Sciences, Australian National University, Canberra, Australian Capital Territory 2601, Australia (A.B.C., M.R.B.); and Australian Research Council Centre of Excellence in Plant Energy Biology and Centre of Excellence for Plant Metabolomics, University of Western Australia, Crawley, Western Australia 6009, Australia (I.P., W.Z., S.M.S.)

Peroxisomes are important for recycling carbon and nitrogen that would otherwise be lost during photorespiration. The reduction of hydroxypyruvate to glycerate catalyzed by hydroxypyruvate reductase (HPR) in the peroxisomes is thought to be facilitated by the production of NADH by peroxisomal malate dehydrogenase (PMDH). PMDH, which is encoded by two genes in Arabidopsis (*Arabidopsis thaliana*), reduces NAD^+ to NADH via the oxidation of malate supplied from the cytoplasm to oxaloacetate. A double mutant lacking the expression of both *PMDH* genes was viable in air and had rates of photosynthesis only slightly lower than in the wild type. This is in contrast to other photorespiratory mutants, which have severely reduced rates of photosynthesis and require high CO_2 to grow. The *pmdh* mutant had a higher O_2-dependent CO_2 compensation point than the wild type, implying that either Rubisco specificity had changed or that the rate of CO_2 released per Rubisco oxygenation was increased in the *pmdh* plants. Rates of gross O_2 evolution and uptake were similar in the *pmdh* and wild-type plants, indicating that chloroplast linear electron transport and photorespiratory O_2 uptake were similar between genotypes. The CO_2 postillumination burst and the rate of CO_2 released during photorespiration were both greater in the *pmdh* mutant compared with the wild type, suggesting that the ratio of photorespiratory CO_2 release to Rubisco oxygenation was altered in the *pmdh* mutant. Without PMDH in the peroxisome, the CO_2 released per Rubisco oxygenation reaction can be increased by over 50%. In summary, PMDH is essential for maintaining optimal rates of photorespiration in air; however, in its absence, significant rates of photorespiration are still possible, indicating that there are additional mechanisms for supplying reductant to the peroxisomal HPR reaction or that the HPR reaction is altogether circumvented.

The oxygenation of ribulose-1,5-bisphosphate by Rubisco initiates the photorespiratory metabolic pathway (Badger, 1985). This reaction competes with photosynthetic carbon assimilation, producing CO_2 and NH_3 while consuming ATP and reducing equivalents, thus minimizing the efficiency of net CO_2 assimilation (Tolbert, 1997; Wingler et al., 2000; Reumann and Weber, 2006). Rates of photorespiration are about 20% of the rate of net CO_2 assimilation in C_3 plants under current ambient CO_2 concentrations at 25°C and thus consume a large portion of the solar energy absorbed by a leaf (Ort and Baker, 2002). The oxygenation reaction yields 3-phosphoglycerate (3-PGA) and 2-phosphoglycolate (2-PG). The 3-PGA is assimilated into the Calvin-Benson cycle, whereas 2-PG cannot enter this cycle directly, nor can it be converted to carbohydrates. To minimize carbon loss and to prevent the depletion of intermediates of the Calvin-Benson cycle, three-quarters of the carbon in 2-PG is recycled by the photorespiratory pathway into 3-PGA, typically releasing one CO_2 per two 2-PG molecules.

The recycling of carbon by the photorespiratory pathway involves at least 11 enzymatic steps that occur in three leaf organelles (chloroplast, mitochondria, and peroxisomes; Reumann and Weber, 2006). The peroxisomes oxidize glycolate, produced in the chloroplast, to glyoxylate by transferring electrons to O_2, thus consuming O_2 and forming hydrogen peroxide (H_2O_2; Reumann, 2000; Mano and Nishimura, 2005). The glyoxylate is further metabolized by two aminotransferases in the peroxisomes, producing Gly,

[1] This work was supported by the Australian Research Council (grant nos. FF0457721 and CE0561495) and the Centres of Excellence Program of the Government of Western Australia.

* Corresponding author; e-mail acousins@wsu.edu.

The author responsible for distribution of materials integral to the findings presented in this article in accordance with the policy described in the Instructions for Authors (www.plantphysiol.org) is: Steven M. Smith (ssmith@cyllene.uwa.edu.au).

[W] The online version of this article contains Web-only data.

[OA] Open Access articles can be viewed online without a subscription.

www.plantphysiol.org/cgi/doi/10.1104/pp.108.122622

which is subsequently processed by the mitochondrion, releasing CO_2 and NH_3 while producing NADH and Ser. It is generally accepted that the Ser returns to the leaf peroxisomes, where the amino group is transferred to glyoxylate, forming Gly and hydroxypyruvate (Reumann and Weber, 2006). The hydroxypyruvate is thought to be reduced to glycerate by hydroxypyruvate reductase (HPR), with NADH being provided by the peroxisomal malate dehydrogenase (PMDH; Reumann and Weber, 2006). The glycerate is phosphorylated within the chloroplast and enters into the Calvin-Benson cycle as 3-PGA.

Mutants of the photorespiratory cycle have provided much to the understanding of this biochemical pathway (Somerville and Ogren, 1982; Leegood et al., 1995; Somerville, 2001; Reumann and Weber, 2006). These mutations generally show chlorotic phenotypes when grown under ambient CO_2 concentrations but are not affected under growth conditions that suppress photorespiration, such as elevated CO_2 (Somerville and Ogren, 1982; Reumann and Weber, 2006). The observed phenotypes have been assumed to be due to the depletion of photosynthetic carbon and nitrogen cycle intermediates and perhaps to the accumulation of toxic photorespiratory intermediates. However, recently, it has become apparent that photorespiratory mutants exposed to air show severe photodamage to PSII due to an inhibition of protein repair processes, linked perhaps to increased oxidative damage to stromal protein synthesis machinery (Takahashi et al., 2007). The original mutant screens searching for chlorosis under ambient CO_2 concentrations primarily identified conditional lethal mutations (plants not viable under long-term exposure to ambient CO_2 concentrations), and more subtle mutations in the photorespiratory pathway were not easily resolved.

However, some subtle mutations in photorespiration do exist; an example of this is peroxisomal HPR, in which a mutant in barley (*Hordeum vulgare*) was selected by screening plants that grew poorly in air. The HPR mutant showed reduced levels of the NADH-dependent peroxisomal HPR activity, but rates of photosynthesis were only reduced by 25% compared with wild-type plants when measured under ambient CO_2 concentrations (Murray et al., 1989). Related mutants lacking PMDH have also been reported in Arabidopsis (*Arabidopsis thaliana*) as growing slower in air, but surviving (Pracharoenwattana et al., 2007). It was proposed that an alternative pathway may metabolize hydroxypyruvate during photorespiration in these mutants, such as a cytosolic HPR or being linked to simultaneous β-oxidation in the peroxisome (Murray et al., 1989; Kleczkowski et al., 1990; Pracharoenwattana et al., 2007). This alternative pathway may provide an overflow metabolic route of hydroxypyruvate reduction if the commonly recognized reaction becomes limiting when rates of photorespiration are high (Murray et al., 1989).

Perturbing the flow of carbon through an alternative photorespiratory pathway has important implications for CO_2 efflux following the Rubisco oxygenation reaction. Evidence strongly indicates that the photorespiratory pathway releases 1 mol of CO_2 for every 2 mol of 2-PG entering the cycle during the conversion of Gly to Ser (Farquhar et al., 1980). However, disruption of the photorespiratory pathway may lead to the accumulation of intermediate compounds, allowing for alternative enzymatic and spontaneous reactions to occur. For example, in barley Gly decarboxylase (GDC) mutants lacking the ability to decarboxylate Gly, the levels of glyoxylate and formate under photorespiratory conditions increased in comparison with those in wild-type plants (Wingler et al., 1999). The production of formate can come from glyoxylate reacting with H_2O_2 nonenzymatically, and the formate can be further incorporated into Ser via the C1-tetrahydrofolate synthase/Ser hydroxymethyl transferase pathway, partially compensating for the lack of GDC activity in these plants (Wingler et al., 1999).

The role of PMDH and the HPR reaction are unclear in photorespiration. In Arabidopsis, two *PMDH* genes have been identified and inactivated either individually or together (Pracharoenwattana et al., 2007). While the *PMDH1* gene is preferentially expressed in seedlings and the *PMDH2* gene is preferentially expressed in leaves, they do appear to be partially redundant (Pracharoenwattana et al., 2007). Mutants containing T-DNA insertions in both *PMDH* genes demonstrate that this enzyme plays an important role in NADH oxidation during fatty acid β-oxidation in germinating seeds (Pracharoenwattana et al., 2007). However, as these plants appeared to grow well in air, this study cast doubt on the role of PMDH during photorespiration and challenged the notion that PMDH provides the NADH required for the reduction of hydroxypyruvate by HPR (Reumann and Weber, 2006). Here, we reanalyzed the Arabidopsis single and double *pmdh* mutants and discovered that these mutations cause subtle changes in the rates of photosynthesis under photorespiratory conditions (ambient CO_2 and O_2 concentrations) and significantly influence the flow of carbon during photorespiration, leading to increased CO_2 released relative to the rates of Rubisco oxygenation reactions.

RESULTS

CO_2 Assimilation Rate, Growth Analysis, and Leaf Characteristics

Rates of net CO_2 assimilation measured at approximately air CO_2 concentrations (373 μbar) in both the wild-type and *pmdh1* plants were significantly higher than in the *pmdh2* and double *pmdh1pmdh2* lines (Table I). However, when rates of net CO_2 assimilation were measured at elevated CO_2 (1,515 μbar), there was no significant difference between the lines (Table I). Stomatal conductance was similar in all genotypes except for the *pmdh2* lines, which had lower stomatal con-

Table I. *Leaf gas-exchange measurements*

The rates of net CO_2 assimilation and stomatal conductance in air (373 μbar) and elevated (1,515 μbar) CO_2 concentrations and the Γ in wild-type plants, peroxisomal NAD^+-malate dehydrogenase 1 and 2 plants (*pmdh1* and *pmdh2*, respectively), and double *pmdh1pmdh2* T-DNA mutants of Arabidopsis. Gas-exchange measurements were made at a pO_2 of 200 mbar, irradiance of 500 μmol quanta m^{-2} s^{-1}, and leaf temperature of 25°C. Values of Γ were inferred from the initial slope of a CO_2 response curve at lowest CO_2 concentrations. Shown are means ± SE of measurements made on three to five leaves from separate plants. Statistical analysis was conducted using ANOVA, and different letters indicate significant differences between plants at $P < 0.05$.

Variable	Wild Type	*pmdh1*	*pmdh2*	*pmdh1pmdh2*
Net CO_2 assimilation rate (μmol CO_2 m^{-2} s^{-1})				
Air	10.6 ± 1.1 a	9.9 ± 1.3 a	8.2 ± 1.3 a,b	6.9 ± 0.4 b
Elevated CO_2	17.5 ± 1.4 a	17.2 ± 2.6 a	14.5 ± 2.9 a	15.2 ± 1.0 a
Stomatal conductance (mmol m^{-2} s^{-1})				
Air	0.20 ± 0.02 a	0.20 ± 0.02 a	0.15 ± 0.02 b	0.20 ± 0.01 a
Elevated CO_2	0.21 ± 0.03 a	0.17 ± 0.03 a	0.13 ± 0.01 b	0.19 ± 0.02 a
Γ (μbar)	59 ± 5 a	65 ± 3 a	81 ± 1 a	109 ± 9 b

ductance values then the other lines under both measurement conditions (Table I). The CO_2 compensation point (Γ), inferred from the initial slope of a CO_2 response curve at lowest CO_2 concentrations, was significantly higher in the *pmdh1pmdh2* plants compared with the other three genotypes (Table I). These data were consistent with variation in compensation points measured for leaf discs in a mass spectrometer closed cuvette compensation point measurement system (data not shown).

The *pmdh1pmdh2* lines grew more slowly in air (as would be expected), as indicated by plant size, and growth analyses showed that growth rate on a leaf area basis was 30% to 40% less than in the wild type (Table II). However, under elevated atmospheric CO_2 concentrations (2.8 mbar), the growth rates of the wild-type and *pmdh1pmdh2* lines were not significantly different (Table II). The growth analysis measurements were conducted during the first 31 d after germination, before the plants were too big for the imaging system. Additionally, there were no significant differences in Rubisco content (μmol site m^{-2}), total leaf nitrogen per area (mmol m^{-2}), and leaf mass per area (g m^{-2}) in the wild-type and *pmdh1pmdh2* lines grown under elevated atmospheric CO_2 (Table II).

The Γ in Response to Oxygen Concentrations

The Γ, as determined from measurements made with the closed leaf chamber coupled to the mass spectrometer (Fig. 1), had a positive relationship with increased oxygen concentration, as predicted from Equation 3 (Fig. 2). Values of Γ were similar in the wild-type and *pmdh1pmdh2* lines at low oxygen (10%), when the rates of photorespiration are expected to be low (see below and Fig. 2); however, Γ was greater in the *pmdh1pmdh2* plants compared with the wild-type plants when measured at the higher oxygen levels (Fig. 2).

O_2 Exchange and Rubisco Reactions at the Γ

The rates of $^{16}O_2$ evolution, $^{18}O_2$ uptake, and net CO_2 exchange were also measured with the leaf discs in a closed system attached to the mass spectrometer (Fig. 1). The rates of CO_2 exchange and $^{18}O_2$ uptake in the dark were similar between the wild-type and *pmdh1pmdh2* plants in response to changing oxygen levels (data not shown). Additionally, measurements of $^{16}O_2$ evolution and $^{18}O_2$ uptake at the compensation point, where net CO_2 exchange is zero, were similar in

Table II. *Growth analysis and leaf characteristics*

The growth rate under ambient CO_2 and elevated atmospheric CO_2 (2.8 mbar) in wild-type and *pmdh1pmdh2* plants. Rubisco content, total leaf nitrogen per area, and leaf mass per area in both genotypes were determined in plants grown under elevated atmospheric CO_2 only. Values shown are means ± SE of measurements made from three to five leaves from separate plants. Statistical analysis was conducted using Student's *t* test, and different letters indicate significant differences between plants at $P < 0.05$.

Variable	Wild Type	*pmdh1pmdh2*
Growth rate in air CO_2 (cm^2 cm^{-2} d^{-1})	0.200 ± 0.045 a	0.125 ± 0.035 b
Growth rate at elevated CO_2 (cm^2 cm^{-2} d^{-1})	0.155 ± 0.014 a	0.137 ± 0.016 a
Rubisco content (μmol site m^{-2})	5.8 ± 1.6 a	6.3 ± 1.0 a
Total leaf nitrogen (mmol m^{-2})	92.2 ± 5.0 a	89.8 ± 6.2 a
Leaf mass per area (g m^{-2})	23.0 ± 1.5 a	21.1 ± 1.7 a

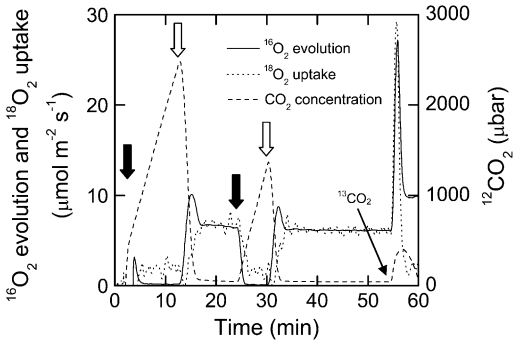

Figure 1. Typical trace of $^{16}O_2$ evolution (solid line), $^{18}O_2$ uptake (dotted line), and CO_2 concentration (dashed line) of a leaf disc in a closed chamber coupled to a mass spectrometer. A leaf disc was placed in the chamber and flushed with nitrogen gas, and a volume of pure oxygen highly enriched in ^{18}O was injected to obtain an O_2 concentration of 10%, 20%, or 40%. After a 10-min dark period, the leaf disc was illuminated (300 μmol quanta m^{-2} s^{-1}) for 10 min, then darkened for 5 min and again illuminated for 10 min. Black arrows indicate lights off, and white arrows indicate lights on. The PIB was determined after the initial 10-min light period, and the parameters relating to the Γ were determined at the end of the final light period. CO_2 enriched in ^{13}C was injected into the leaf chamber to saturate photosynthesis in the light, and the rates of photorespiratory CO_2 release were estimated from the rate of $^{12}CO_2$ released during this time period.

the wild-type and *pmdh1pmdh2* plants at both 10% and 20% oxygen (Fig. 3, A and B). However, $^{16}O_2$ evolution and $^{18}O_2$ uptake were significantly lower in the *pmdh1pmdh2* plants compared with the wild-type plants at the highest oxygen levels (40%; Fig. 3, A and B). The rates of Rubisco oxygenation (v_o) and carboxylation (v_c) reactions at the Γ were determined using Equations 1 and 2, respectively (see "Materials and Methods"). The values of v_o and v_c were similar between the wild-type and *pmdh1pmdh2* plants at 10% and 20% oxygen (Fig. 3, C and D). However, similar to the rates of $^{16}O_2$ evolution and $^{18}O_2$ uptake, the rates of v_o and v_c were lower in the *pmdh1pmdh2* plants compared with the wild-type plants at 40% oxygen (Fig. 3, C and D).

Postillumination Burst and Photorespiratory Release of CO_2

The postillumination burst (PIB), determined by turning off the light and monitoring the rapid efflux of $^{12}CO_2$ in the dark after an initial 10-min period in the light, was significantly higher in the *pmdh1pmdh2* plants compared with the wild-type plants at 20% and higher oxygen levels (Fig. 4A). The values of PIB measured at low oxygen (10%) were similar in the wild-type and *pmdh1pmdh2* plants (Fig. 4A). The photorespiratory release of CO_2 was determined by injection of CO_2 enriched in ^{13}C into the leaf chamber to saturate the rates of the Rubisco carboxylation reaction in the light and subsequently monitoring the rates of photorespiratory $^{12}CO_2$ release. The release was greater in the *pmdh1pmdh2* plants compared with the wild-type plants at 20% and higher oxygen levels but not at 10% oxygen (Fig. 4B). The ratio of PIB to the rate of v_o as well as the ratio of photorespiratory CO_2 release to v_o were higher in the *pmdh1pmdh2* plants compared with the wild-type plants at 20% and 40% oxygen but not at 10% oxygen (Fig. 4, C and D).

Metabolite Analysis

Leaf discs were harvested after 10 min at the Γ and extracts subjected to gas chromatography-mass spectrometry (GC-MS) analysis. Relative amounts of numerous primary metabolites that were identified reliably were compared (Supplemental Table S1). Several photorespiratory intermediates were detected by this method, but differences in relative amounts between *pmdh1pmdh2* and the wild type were no more than 1.6-fold. Glycolate, glyoxylate, Glu, and glycerate were unchanged in amount, while Gln and Asp were marginally lower and malate, Gly, and Ser were marginally higher. The method employed did not detect hydroxypyruvate or oxaloacetate.

DISCUSSION

The Role of PMDH

It is apparent that PMDH activity is not essential for photosynthesis in air in Arabidopsis. However, it is necessary for optimal rates of photosynthesis and growth in air (Tables I and II). The explanation for how the photorespiratory pathway functions without

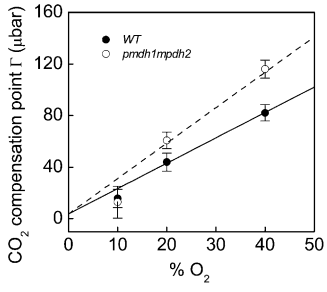

Figure 2. The Γ at different O_2 partial pressures in the wild type and the *pmdh1pmdh2* double mutant. Measurements were made in a closed leaf chamber coupled to a mass spectrometer as described for Figure 1. The lines represent the theoretical relationship between Γ and O_2 partial pressure:

$$\Gamma = \frac{\Gamma^* + K_c(1 + O/K_o)R_d/V_{cmax}}{1 - R_d/V_{cmax}} \quad (3)$$

where $\Gamma^* = \alpha(V_{omax}K_cO)/(V_{cmax}K_o)$, α is the ratio of CO_2 released per oxygenation reaction (0.5 for the solid line and 0.8 for the dotted line), O is the O_2 partial pressure, K_c = 258 μbar and K_o = 171 mbar are the Michaelis-Menten constants of Rubisco carboxylation and oxygenation, V_{omax}/V_{cmax} = 0.255, and R_d/V_{cmax} = 0.01 (Ruuska et al., 2000). Data are means of measurements of three to five different plants, and error bars represent SE.

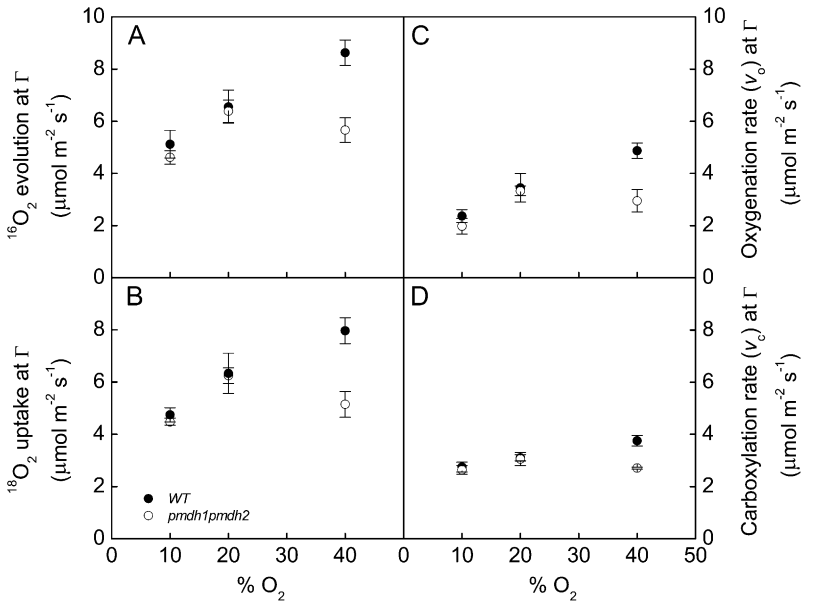

Figure 3. Oxygen exchange. $^{16}O_2$ evolution (A), $^{18}O_2$ uptake (B), v_o (C), and v_c (D) rates at the Γ at different O_2 partial pressures in wild-type (black symbols) and *pmdh1pmdh2* (white symbols) plants. Data are means of measurements of three to five different plants, and error bars represent SE. Calculation of v_o [2/3($^{18}O_2$ uptake in light − $^{18}O_2$ uptake in dark)] and v_c [$^{16}O_2$ evolution − v_o] were determined from mass spectrometer measurements of O_2 as presented in Figure 2.

PMDH activity in air may lie in two areas: first, the potential sources of reductant for the HPR reaction; second, the ability of hydroxypyruvate to be processed by alternative reactions either in the peroxisome or the cytosol.

It is widely accepted that the PMDH provides reductant in the form of NADH to facilitate the reduction of hydroxypyruvate by HPR (Reumann and Weber, 2006). The peroxisomal membrane is assumed to be impermeable to NADH (Donaldson, 1982; Vanroermund et al., 1995; Reumann and Weber, 2006), and the NADH required within the peroxisomes must be synthesized in situ. Traditionally, the malate/oxaloacetate shuttle across the peroxisomal membrane is believed to supply malate derived from either the chloroplast or the mitochondrion to facilitate the reduction of NAD^+ to NADH via PMDH. Additionally, β-oxidation of fatty acids results in the reduction of NAD^+ to NADH within the peroxisomes (Pracharoenwattana et al., 2007). However, under ambient air conditions, the NADH produced by β-oxidation would presumably be insufficient to meet the requirement of photorespiratory NADH consumption in a typical C_3 plant. Here, we show that of the two genes known to encode PMDHs, it appears that *PMDH2* has a more dominant role in photorespiration (Table I), as predicted by RNA coexpression analysis (Reumann and Weber, 2006). However, in the double mutant *pmdh1pmdh2* lacking the expression of both *PMDH* genes, the rate of net CO_2 assimilation was still 70% of the wild-type rate under ambient CO_2 and O_2 concentrations during the measurement conditions.

Previous studies of a barley HPR mutant (Murray et al., 1989) also found that although the peroxisomal HPR step was apparently blocked, photosynthesis at air CO_2 concentrations was only reduced by 20% to 30%. This study concluded that an alternative NADPH-dependent HPR pathway based in the cytosol may metabolize a portion of the hydroxypyruvate (Fig. 5). However, preliminary studies indicate that extracts prepared from leaves of an Arabidopsis *hpr* knockout mutant have negligible rates of HP reduction with either NADH or NADPH (I. Pracharoenwattana, unpublished data). In addition to this possibility, the oxidation of hydroxypyruvate to glycolate by nonenzymatic reaction with H_2O_2 (see below and Fig. 5) may also play a role.

Growth and Leaf Analysis

As in other photorespiratory mutants, the growth rates at high CO_2 were similar between the wild-type and *pmdh1pmdh2* plants (Table II). Additionally, the amount of Rubisco, the leaf mass per area, and the total leaf nitrogen were similar in wild-type and *pmdh1pmdh2* plants grown under elevated CO_2 (Table II). These similarities between wild-type and *pmdh1pmdh2* plants under high CO_2 growth conditions are important because they indicate that the differences in photosynthetic and photorespiratory parameters in air between the genotypes are based on metabolic differences during the measurement conditions and are not due to prior growth conditions. This is particularly important with regard to Rubisco content, as will be further discussed below.

Γ and the Response to Oxygen Availability

The Γ, in the presence of mitochondrial respiration, increased with oxygen concentration in both wild-type and *pmdh1pmdh2* plants (Fig. 2). However, Γ was higher in the *pmdh1pmdh2* plants compared with the wild-type plants at ambient and higher oxygen concentrations, where the rates of photorespiration would be high (Table I; Fig. 2). There are several factors that can potentially influence Γ, as shown in Equation 3 in Figure 2. For

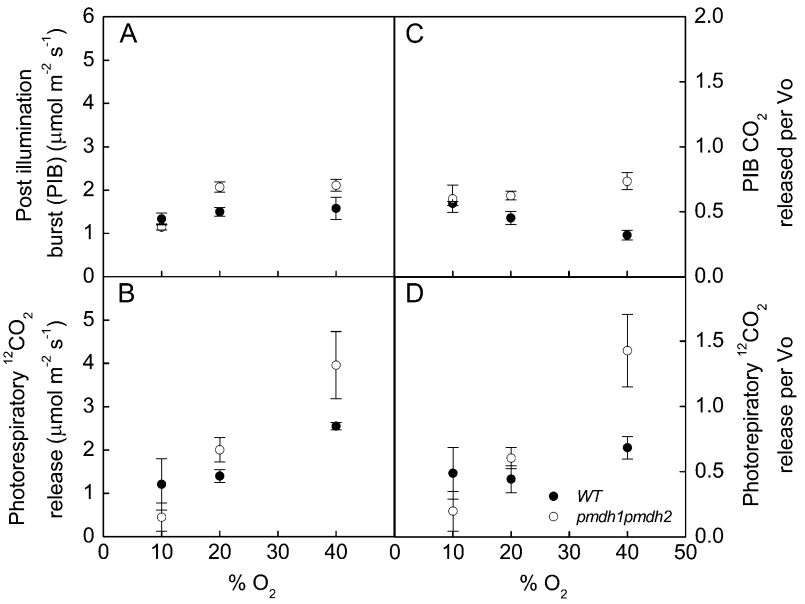

Figure 4. Changes in photorespiratory CO_2 release per Rubisco oxygenation. The PIB (A), the photorespiratory release of CO_2 (B), the PIB relative to the rate of v_o (C), and the photorespiratory release of CO_2 relative to v_o (D) at different O_2 partial pressures in wild-type (black symbols) and *pmdh1pmdh2* (white symbols) plants. Data are means of measurements of three to five different plants, and error bars represent SE.

example, Γ is influenced by the Rubisco Michaelis-Menten constants for CO_2 and O_2, K_c and K_o, respectively, and the maximal rates of Rubisco carboxylation (V_{cmax}) and oxygenation (V_{omax}) reactions, as shown in Equation 3. These parameters determine the CO_2/O_2 specificity of Rubisco ($S_{c/o}$), the ratio of the carboxylase to oxygenase rate at equal CO_2 and O_2 concentrations, as described by $S_{c/o} = (V_{cmax}/K_c)(K_o/V_{omax})$ (von Caemmerer, 2000). These kinetic values, and subsequently $S_{c/o}$, vary between species but are generally considered constant within an individual organism even when grown under different environmental conditions (Jordan and Ogren, 1981). The ratio of respiration (R_d) in the light to V_{cmax} (R_d/V_{cmax}) can also influence values of Γ, as demonstrated in tobacco (*Nicotiana tabacum*) plants, which had reduced amounts of Rubisco but similar rates of R_d (Ruuska et al., 2000). Here, the wild-type and *pmdh1pmdh2* plants had similar rates of respiration in the dark (data not shown) and similar amounts of total Rubisco (Table II). Additionally, the rates of v_o and v_c were similar at 20% and lower oxygen concentrations, as estimated from the leaf O_2 exchange at the Γ (Fig. 3, C and D). Assuming that respiration in the dark is similar to R_d, these data indicate that the increased values of Γ in *pmdh1pmdh2* at 20% O_2 were not related to changes in $S_{c/o}$ or alterations in the ratio R_d/V_{cmax}.

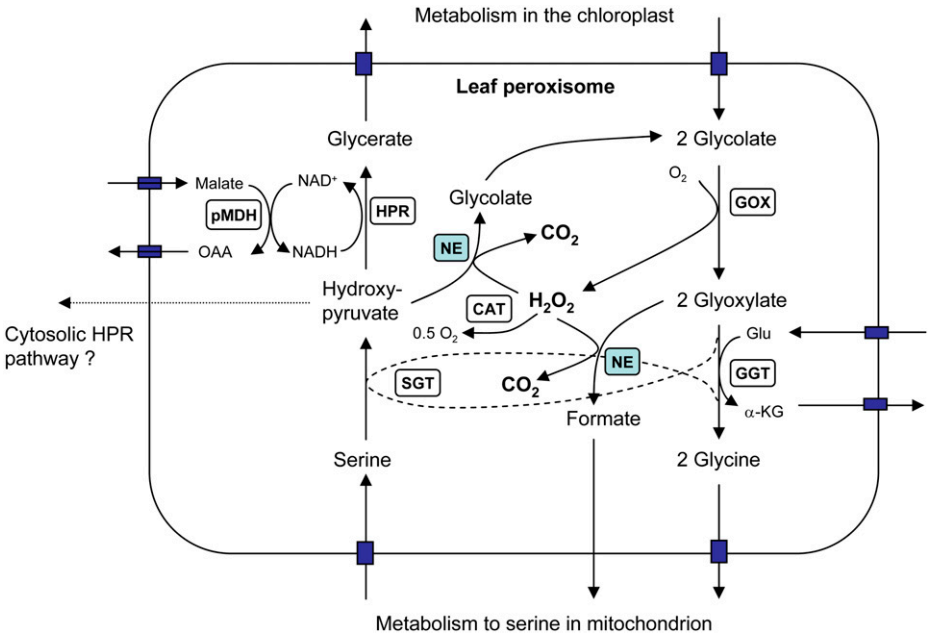

Figure 5. The path of carbon and CO_2 release in the peroxisome. Reactions in the central part of the scheme highlight the potential for H_2O_2 to nonenzymatically (NE) interact with glyoxylate and hydroxypyruvate. Enzymatic steps shown are as follows: CAT, catalase; GGT, Gln:glyoxylate aminotransferase; GOX, glycolate oxidase; SGT, Ser:glyoxylate aminotransferase. A potential pathway for hydroxypyruvate metabolism in the cytosol is indicated. OAA, Oxaloacetate; α-KG, α-ketoglutarate.

In addition to the above parameters, values of Γ are also influenced by Γ*, the Γ in the absence of respiration (Fig. 2, Eq. 3). Values of Γ* are estimated as $\Gamma^* = \alpha(V_{omax}K_cO)/(V_{cmax}K_o)$, where α is the ratio of CO_2 released per oxygenation reaction and O is the oxygen concentration. As described in the following section and in Figure 2, changes in α can have a significant effect on Γ, especially when rates of photorespiration are high.

Photorespiratory CO_2 Release per Oxygenation Reaction

During photorespiration, 1 mol of 2-PG is assumed to release 0.5 mol of CO_2 during the conversion of Gly to Ser; therefore, the value of $\alpha = 0.5$ (Farquhar et al., 1980; von Caemmerer and Farquhar, 1981). As shown in Figure 2, changes in α can have a large effect on the predicted Γ values. For example, at 20% O_2, changing α from 0.5 to 0.8 increases the predicted value of Γ from 38 to 62 μbar, and the effect is greater at higher O_2 concentrations (Fig. 2). The predicted Γ values in Figure 2 when $\alpha = 0.5$ (solid line) describes the response of Γ to increasing O_2 concentration in the wild-type plants but underestimates Γ in the *pmdh1pmdh2* plants. However, when changing α to 0.8 in Equation 3 (Figure 2, dashed line), the theoretical estimates of Γ in response to O_2 fit the measured values of Γ in the *pmdh1pmdh2* plants (Fig. 2).

The rates of O_2 uptake and evolution, measured at the Γ with the mass spectrometer, were similar in wild-type and *pmdh1pmdh2* plants at 20% and lower O_2 concentrations (Fig. 3, A and B). At 40% O_2, at which photorespiration would be higher, the rates of O_2 uptake and evolution were significantly lower in the *pmdh1pmdh2* plants compared with the wild-type plants (Fig. 3, A and B). This is likely because at 40% O_2, the unidentified alternative photorespiratory pathway utilized by the *pmdh1pmdh2* plants is insufficient to keep up with the recycling of photorespiratory intermediates of the Calvin-Benson cycle, and Rubisco activity either becomes ribulose-1,5-bisphosphate limited or inhibited by the increased levels of photorespiratory intermediates (Wingler et al., 2000). The lower rates of v_o and v_c in the *pmdh1pmdh2* plants compared with wild-type plants at 40% O_2 further support the idea that Rubisco activity becomes inhibited at the highest O_2 concentration in the *pmdh1pmdh2* plants (Fig. 3, C and D).

We used two techniques to investigate the relationship of the ratio of photorespiratory CO_2 released per oxygenation reaction. In the first method, we monitored the PIB of CO_2 in the dark from the leaf tissue after measuring O_2 and CO_2 exchange at the Γ for 10 min (Fig. 1). These experiments were conducted on the mass spectrometer, where net CO_2 exchange, O_2 evolution, O_2 uptake, and O_2 concentrations were simultaneously determined (Figs. 1 and 4). The PIB represents the CO_2 released by the photorespiratory cycle after the oxygenation and carboxylation reactions have ceased after turning off the light. Figure 4A shows that the PIB was higher in the *pmdh1pmdh2* plants compared with the wild-type plants at the higher O_2 concentrations, indicating that there is a greater release of photorespiratory CO_2 per glycolate molecule in the *pmdh1pmdh2* plants compared with the wild-type plants. The photorespiratory pathway will continue to function after the light has been turned off until the pools of photorespiratory intermediates produced in the light period have been consumed (Laisk and Edwards, 1997; Hoefnagel et al., 1998; Atkin et al., 2000). Therefore, the peak rate of CO_2 released during the PIB is an indicator of the rate of CO_2 produced during photorespiration prior to darkening. In the traditional view of photorespiration, the CO_2 released is primarily produced from the conversion of Gly to Ser by GDC within the mitochondria, but it is not a specific measure of α. However, in the *pmdh1pmdh2* plants and other photorespiratory mutants, such as the GDC barley mutant, the PIB will also measure other decarboxylating reactions associated with the altered photorespiratory pathways.

Additionally, the export of Ser and/or Gly via the vascular system (Madore and Grodzinski, 1984; Wingler et al., 2000) or the involvement of Ser/Gly in one-carbon metabolism and protein synthesis (Hanson and Roje, 2001) would alter the flow of carbon through the photorespiratory cycle. If large quantities of Gly were lost from the photorespiratory cycle, due to alternative metabolism or export to vascular tissue, this would decrease α and thus Γ, since the amount of CO_2 released per Rubisco oxygenation reaction would approach zero. Alternatively, the catabolism of Gly through C1 metabolism could potentially increase α if the stoichiometry was greater than 0.5 CO_2 released per Gly molecule. However, Gly does not appear to be used directly for C1 metabolism but is first converted to Ser through GDC and Ser hydroxymethyltransferase reactions (Mouillon et al., 1999). Alternatively, if large quantities of Ser were diverted out of the photorespiratory cycle, there would be no effect on α, as the release of CO_2 due to the conversion of Gly to Ser would be conserved. Although the potential for Ser and/or Gly loss from the photorespiratory cycle cannot be excluded, it does not fit with the increase in Γ seen in the *pmdh1pmdh2* mutant.

The second method of estimating the release of CO_2 during photorespiration was to take advantage of the mass spectrometer's ability to measure CO_2 isotopologues, $^{12}CO_2$ and $^{13}CO_2$, simultaneously. After the rates of O_2 and $^{12}CO_2$ exchange were measured at the Γ for 10 min (Fig. 1), a volume of $^{13}CO_2$ was injected into the leaf chamber to saturate the rates of v_c and eliminate the v_o reaction. By monitoring the release of $^{12}CO_2$ directly after the injection of $^{13}CO_2$, the rates of CO_2 released by photorespiration prior to the $^{13}CO_2$ injection can be estimated in the light without darkening. The rates of CO_2 released during photorespiration determined from this method were also greater in the *pmdh1pmdh2* plants compared with the wild-type plants (Fig. 4B).

Both the PIB and $^{13}CO_2$ techniques show that the rates of photorespiratory release of CO_2 were greater in the *pmdh1pmdh2* plants compared with the wild-type plants (Fig. 4, A and B). This indicates that either the *pmdh1pmdh2* plants had greater rates of photorespiration or that the amount of CO_2 released per oxygenation reaction was greater compared with that in the wild-type plants. At 20% oxygen, the measured rates of v_o were similar in both genotypes (Fig. 3C), and the ratio of photorespiratory CO_2 release per Rubisco oxygenation reaction in the *pmdh1pmdh2* plants was higher compared with the wild-type plants using both methods of determining photorespiratory CO_2 (Fig. 4, C and D). This supports the predicted higher α values in the *pmdh1pmdh2* plants compared with the wild-type plants, as presented in Figure 2.

Photorespiratory Metabolites

Overall, the metabolite analysis did not provide any evidence for major perturbation of photorespiratory metabolism (Supplemental Table S1). The small increases in Gly and Ser are consistent with a block downstream at the PMDH step, while decreases in Gln and Asp are consistent with less efficient ammonia reassimilation. It is intriguing 2-ketoglutaric acid and isocitrate increased, by 3.6- and 7.5-fold, respectively, in the *pmdh1pmdh2* plants compared with the wild-type plants (Supplemental Table S1). This may suggest that the altered consumption of reductant (NADH) in the peroxisomes due to the lack of PMDH caused the NADH/NAD ratio in the mitochondria to increase. An increase in mitochondrial NADH/NAD has been demonstrated to inhibit the NAD-dependent isocitrate dehydrogenase (Igamberdiev and Gardestrom, 2003) and may explain the relatively large increase in isocitrate in the *pmdh1pmdh2* plants. The increase in 2-oxoglutarate could potentially be attributed to an alteration in the Glu requirement for recycling nitrogen through the GS/GOGAT-catalyzed reactions. However, a full evaluation of the metabolic basis for the greater CO_2 release in the absence of PMDH will require more detailed analysis in the future.

How Is the Stoichiometry of CO_2 Release Altered?

The data reported here with the *pmdh1pmdh2* mutant clearly show that some restrictions to the photorespiratory pathway can lead to changes in the pathway of carbon and photorespiratory CO_2 release. Indeed, the results here represent the most dramatic demonstration of this reported in the literature. Studies on various photorespiratory mutants have not consistently agreed on the way that potential CO_2 release steps may be altered. Studies with a barley mutant deficient in Ser:glyoxylate aminotransferase demonstrated significantly elevated release of labeled CO_2 from exogenously supplied glyoxylate (Murray et al., 1987). In contrast, a HPR barley mutant (Murray et al., 1987) showed little evidence for an increased CO_2 release, even though there was considerable photosynthesis in air. A barley mutant deficient in catalase (Kendall et al., 1983) showed no evidence for increased CO_2 release, while an Arabidopsis transgenic plant with antisense reduction in the levels of the 2-oxoglutarate/malate translocator (Schneidereit et al., 2006) showed a significant increase in Γ.

Based on previous studies, the most obvious explanation for an increased CO_2 release stoichiometry would be an alternative oxidative decarboxylation of accumulating pools of glyxoylate and hydroxypyruvate through their nonenzymatic interactions with H_2O_2 to produce formate and glycolate, respectively, plus CO_2 (Halliwel, 1974; Halliwel and Butt, 1974; Grodzinski, 1979; Walton and Butt, 1981; Wingler et al., 1999). In addition, the resulting formate can also be decarboxylated in the peroxisomes by its oxidation via catalase and H_2O_2 (Halliwel and Butt, 1974) or can be oxidized to CO_2 by formate dehydrogenase in the mitochondrion (Hourton-Cabassa et al., 1998). These potential reactions are shown in Figure 5. The potential for these alternative decarboxylations to occur would increase under conditions in which both glyoxylate and hydroxypyruvate accumulate, as would be expected for the *pmdh1pmdh2* mutant described here. Only mutations inactivating PMDH, HPR, or glycerate processing steps would be expected to elevate hydroxypyruvate. Most of the previously studied photorespiratory mutants are blocked in earlier steps, and it is possible that the large increased in CO_2 release stoichiometry observed here may be due to the greater potential for hydroxypyruvate decarboxylation and glycolate recycling in the peroxisome (Walton and Butt, 1981).

CONCLUSION

The peroxisomal NAD^+-malate dehydrogenase 2 (*pmdh2*) appears to play a more prominent role than the peroxisomal NAD^+-malate dehydrogenase 1 (*pmdh1*) during photorespiration. Rates of photosynthesis in air were reduced in the double *pmdh1pmdh2* mutant, but by only 30%. The rates of gross O_2 evolution and uptake were similar in *pmdh1pmdh2* and wild-type plants, indicating that chloroplast linear electron transport and photorespiratory O_2 uptake by Rubisco were similar between genotypes. The CO_2 PIB and the rate of CO_2 released during photorespiration were both greater in the *pmdh1pmdh2* mutant compared with the wild-type plants, suggesting that the ratio of photorespiratory CO_2 release to Rubisco oxygenation was altered in the mutant. In summary, PMDH is essential for maintaining optimal rates of photorespiration in air; however, in its absence, significant rates of photorespiration are still possible, indicating that there are additional mechanisms for supplying reductant to the peroxisomal HPR reaction or that the HPR reaction is altogether circumvented.

MATERIALS AND METHODS

Growth Conditions

Arabidopsis (*Arabidopsis thaliana*) seeds were surface sterilized, stratified, and allowed to imbibe on wet filter paper. Seeds were germinated on half-strength Murashige and Skoog medium with 1% (w/v) Suc and then transferred to potting soil (Debco seedling raising mix). For the gas-exchange measurements and the high-CO_2 growth analysis, plants were grown under 2.8 mbar of CO_2 in a controlled-environment growth cabinet at an irradiance of 200 μmol quanta m^{-2} s^{-1} at plant height, and air temperature of 25°C during the day and 15°C at night, with a daylength of 14 h. Wild-type and *pmdh1pmdh2* plants used for the growth analysis under ambient CO_2 concentrations were grown during the southern hemisphere's autumn month of May in a glasshouse under natural light conditions (25°C day and 15°C night temperatures). For all plants, 0.9-L pots were used, and the potting soil was mixed with 2.4 to 4 g Osmocote/L soil (15:4.8:10.8:1.2 nitrogen:phosphorus: potassium:magnesium + trace elements: boron, copper, iron, manganese, molybdenum, and zinc; Scotts Australia) and watered daily.

Gas-Exchange Measurements

Measurements of Net CO_2 Assimilation Rates

Individual plants were brought from the growth chambers into the laboratory, and a single leaf was dark adapted for 30 min in the LI6400 (LiCor Biosciences) leaf chamber (LI6400-40). Gas-exchange measurements were made at pO_2 of 200 mbar, irradiance of 500 μmol quanta m^{-2} s^{-1}, and leaf temperature of 25°C. The Γ measurements shown in Table I were inferred from the initial slope of a CO_2 response curve at lowest CO_2 concentrations. All other values of Γ were measured on the mass spectrometer as described below.

Mass Spectrometric Measurements

The exchange of O_2 and CO_2 was measured from leaf discs placed into a closed leaf chamber attached to a mass spectrometer (Isoprime Micromass) as described previously (Maxwell et al., 1998; Ruuska et al., 2000). After the leaf disc was placed in the chamber, the chamber was flushed with nitrogen gas and a volume of pure oxygen enriched in ^{18}O was injected to obtain an O_2 concentration of 10%, 20%, or 40%. After a 10-min dark period, the leaf disc was illuminated (300 μmol quanta m^{-2} s^{-1}) for 10 min, then darkened for 5 min, and again illuminated for 10 min (Fig. 1). The PIB was determined after the initial 10-min light period, and the parameters relating to the Γ were determined at the end of the final light period. CO_2 enriched in ^{13}C ($^{13}CO_2$; 99% enrichment) was injected into the leaf chamber to saturate the rates of the Rubisco carboxylation reaction in the light. The PIB and the photorespiratory CO_2 release in the light were estimated from the rate of $^{12}CO_2$ released. The rate of CO_2 release was calculated from the $^{12}CO_2$ concentration signal by measuring the slope of a moving five-point window (10-s width) over the data during this time period, and the peak values for rates were determined. To correct for the contamination of $^{12}CO_2$ during the injection of $^{13}CO_2$, several injections were conducted with an empty leaf chamber throughout each day that measurements were conducted. The background $^{12}CO_2$ increase during the blank injection was subtracted from the data collected during the measurement with the leaf disc enclosed in the chamber.

Growth Analysis

Growth analyses were done on a leaf area expansion basis by nondestructively measuring the displayed leaf area of individual plants at time intervals. Total leaf area (including petioles) was measured by imaging the chlorophyll fluorescence (CF Imager; Technologica) and using the leaf area function available for total fluorescent pixels of each plant. The area was calibrated against a known image standard. Leaf area expansion rates are calculated from the slope of ln(area) versus time in units of cm^2 cm^{-2} d^{-1}, and means and SE values are reported for four to five separate plants imaged over a 7- to 10-d time course during the exponential growth phase of each seedling. Imaging commenced at approximately 22 d after sowing.

Metabolite Analysis

Plant tissues (10–30 mg) were snap frozen and pulverized in liquid nitrogen. The enzymes in the tissue were inactivated by heating at 70°C for 15 min in 500 μL of extraction solution (methanol:water = 20:3, with adipic acid as internal standard). Cells debris was removed by centrifugation. For each sample, 60 μL of supernatant was transferred to a new tube and dried using a SpeedVac. The residue was dissolved in 20 μL of pyridine with methoxylamine hydrochloride (20 mg mL^{-1}) and incubated at 30°C for 90 min with shaking. Metabolites were converted to *tert*-butyldimethylsilyl derivatives by reacting at 70°C for 30 min with 30 μL of *N*-methyl-*N*-[*tert*-butyldimethylsilyl]trifluoroacetimide plus 1% *tert*-butyldimetheyl-chlorosilane. The metabolite derivatives were analyzed by GC-MS (Agilent 6890 gas chromatograph coupled with a 5973N mass selective detector). GC-MS data were processed by AMDIS. Metabolite derivatives were identified by comparison of the retention time and mass spectra of authentic standards, and the amount of metabolites was calculated by total ion current signal of each metabolite peak normalized to the internal standard and tissue weight.

Rubisco Content

The content of Rubisco catalytic sites was measured by stoichiometric binding of [^{14}C]carboxy-arabinitol-P_2, and its carbamylation status was measured by exchanging [^{14}C]carboxy-arabinitol-P_2 loosely bound at uncarbamylated sites with an excess of unlabeled C-carboxy-arabinitol-P_2 (Ruuska et al., 1998). Leaf tissue was ground on ice in 600 mL of extraction buffer (50 mM EPPS [4-2(2-hydroxyethyl)-1-piperazine propane sulfonic acid], pH 8.1, 1% polyvinylpolypyrrolidone, 1 mM EDTA, 10 mM dithiothreitol, and 0.1% Triton) with 20 μL of protease inhibitor cocktail (Sigma) and briefly centrifuged.

Calculations of v_o and v_c from MS Measurements

The calculations used were described previously (Ruuska et al., 2000). For each oxygenation reaction of Rubisco, 1 mol of O_2 is consumed, and a further 0.5 mol of O_2 is consumed during photorespiration by glycolate oxidase in the peroxisomes. We assume that O_2 uptake by PSI via the Mehler reaction is negligible and that O_2 uptake by mitochondria was the same in the light and dark. Therefore, v_o was calculated as:

$$v_o = {}^2/_3(^{18}O_2 \text{ uptake in light} - {}^{18}O_2 \text{ uptake in dark}) \quad (1)$$

If the whole chain electron transport results in NADPH production for photosynthesis and photorespiration, then v_c can be calculated as:

$$v_c = {}^{16}O_2 \text{ evolution} - v_o \quad (2)$$

Statistical Analysis

ANOVA was conducted using Student's *t* test in Statistica (version 6.0; StatSoft). Tukey's LSD test was used for post hoc comparisons.

Supplemental Data

The following materials are available in the online version of this article.

Supplemental Table S1. Relative amounts of numerous primary metabolites that were identified reliably with GC-MS. Leaf material was harvested after 10 min at the Γ.

ACKNOWLEDGMENTS

We thank Dave Zeelenberg for running the metabolite analysis and Steve Clayton for total nitrogen analysis. Additionally, A.B.C. thanks Susanne von Caemmerer for many helpful discussions.

Received May 7, 2008; accepted July 26, 2008; published August 6, 2008.

LITERATURE CITED

Atkin OK, Millar AH, Gardestrom P, Day DA (2000) Photosynthesis, carbohydrate metabolism and respiration in leaves of higher plants. *In*

RC Leegood, TD Sharkey, S von Caemmerer, eds, Photosynthesis: Physiology and Metabolism, Vol 9. Kluwer Academic Publishers, Dordrecht, The Netherlands, pp 153–185

Badger M (1985) Photosynthetic oxygen exchange. Annu Rev Plant Physiol **36:** 27–53

Donaldson RP (1982) Nicotinamide cofactors (NAD and NADP) in glyoxysomes, mitochondria, and plastids isolated from castor bean endosperm. Arch Biochem Biophys **215:** 274–279

Farquhar GD, von Caemmerer S, Berry JA (1980) A biochemical model of photosynthetic CO_2 assimilation in leaves of C_3 species. Planta **149:** 78–90

Grodzinski B (1979) Study of formate production and oxidation in leaf peroxisomes during photo-respiration. Plant Physiol **63:** 289–293

Halliwel B (1974) Oxidation of formate by peroxisomes and mitochondria from spinach leaves. Biochem J **138:** 77–85

Halliwel B, Butt VS (1974) Oxidative decarboxylation of glycollate and glyoxylate by leaf peroxisomes. Biochem J **138:** 217–224

Hanson AD, Roje S (2001) One-carbon metabolism in higher plants. Annu Rev Plant Physiol Plant Mol Biol **52:** 119–137

Hoefnagel MHN, Atkin OK, Wiskich JT (1998) Interdependence between chloroplasts and mitochondria in the light and the dark. Biochim Biophys Acta **1366:** 235–255

Hourton-Cabassa C, Ambard-Bretteville F, Moreau F, de Virville JD, Remy R, des Francs-Small CC (1998) Stress induction of mitochondrial formate dehydrogenase in potato leaves. Plant Physiol **116:** 627–635

Igamberdiev AU, Gardestrom P (2003) Regulation of NAD- and NADP-dependent isocitrate dehydrogenases by reduction levels of pyridine nucleotides in mitochondria and cytosol of pea leaves. Biochim Biophys Acta **1606:** 117–125

Jordan DB, Ogren WL (1981) Species variation in the specificity of ribulose-biphosphate carboxylase-oxygenase. Nature **291:** 513–515

Kendall AC, Keys AJ, Turner JC, Lea PJ, Miflin BJ (1983) The isolation and characterization of a catalase-deficient mutant of barley (Hordeum vulgare L). Planta **159:** 505–511

Kleczkowski LA, Randall DD, Zahler WL (1990) Adenylate kinase from maize leaves: true substrates, inhibition by P-1,P-5-di(adenosine-5′) pentaphosphate and kinetic mechanism. Z Naturforsch [C] **45:** 607–613

Laisk A, Edwards GE (1997) Post-illumination CO_2 exchange and light-induced CO_2 bursts during C-4 photosynthesis. Aust J Plant Physiol **24:** 517–528

Leegood R, Lea P, Adcock M, Hausler R (1995) The regulation and control of photorespiration. J Exp Bot **46:** 1397–1414

Madore M, Grodzinski B (1984) Effect of oxygen concentration on C-14-photoassimilate transport from leaves of *Salvia splendens* L. Plant Physiol **76:** 782–786

Mano S, Nishimura M (2005) Plant peroxisomes. Vitam Horm **72:** 111–154

Maxwell K, Badger MR, Osmond CB (1998) A comparison of CO_2 and O_2 exchange patterns and the relationship with chlorophyll fluorescence during photosynthesis in C_3 and CAM plants. Aust J Plant Physiol **25:** 45–52

Mouillon JM, Aubert S, Bourguignon J, Gout E, Douce R, Rebeille F (1999) Glycine and serine catabolism in non-photosynthetic higher plant cells: their role in C1 metabolism. Plant J **20:** 197–205

Murray AJS, Blackwell RD, Joy KW, Lea PJ (1987) Photorespiratory-N donors, aminotransferase specificity and photosynthesis in a mutant of barley deficient in serine-glyoxylate aminotransferase activity. Planta **172:** 106–113

Murray AJS, Blackwell RD, Lea PJ (1989) Metabolism of hydroxypyruvate in a mutant of barley lacking NADH-dependent hydroxypyruvate reductase, an important photorespiratory enzyme activity. Plant Physiol **91:** 395–400

Ort DR, Baker NR (2002) A photoprotective role for O_2 as an alternative electron sink in photosynthesis? Curr Opin Plant Biol **5:** 193–198

Pracharoenwattana I, Cornah JE, Smith SM (2007) Arabidopsis peroxisomal malate dehydrogenase functions in beta-oxidation but not in the glyoxylate cycle. Plant J **50:** 381–390

Reumann S (2000) The structural properties of plant peroxisomes and their metabolic significance. Biol Chem **381:** 639–648

Reumann S, Weber APM (2006) Plant peroxisomes respire in the light: some gaps of the photorespiratory C_2 cycle have become filled—others remain. Biochim Biophys Acta **1763:** 1496–1510

Ruuska S, Andrews TJ, Badger MR, Hudson GS, Laisk A, Price GD, von Caemmerer S (1998) The interplay between limiting processes in C_3 photosynthesis studied by rapid-response gas exchange using transgenic tobacco impaired in photosynthesis. Aust J Plant Physiol **25:** 859–870

Ruuska S, Badger MR, Andrews TJ, von Caemmerer S (2000) Photosynthetic electron sinks in transgenic tobacco with reduced amounts of Rubisco: little evidence for significant Mehler reaction. J Exp Bot **51:** 357–368

Schneidereit J, Hausler RE, Fiene G, Kaiser WM, Weber APM (2006) Antisense repression reveals a crucial role of the plastidic 2-oxoglutarate/malate translocator DiT1 at the interface between carbon and nitrogen metabolism. Plant J **45:** 206–224

Somerville CR (2001) An early Arabidopsis demonstration: resolving a few issues concerning photorespiration. Plant Physiol **125:** 20–24

Somerville CR, Ogren WL (1982) Genetic modification of photorespiration. Trends Biochem Sci **7:** 171–174

Takahashi S, Bauwe H, Badger M (2007) Impairment of the photorespiratory pathway accelerates photoinhibition of photosystem II by suppression of repair but not acceleration of damage processes in Arabidopsis. Plant Physiol **144:** 487–494

Tolbert NE (1997) The C_2 oxidative photosynthetic carbon cycle. Annu Rev Plant Physiol Plant Mol Biol **48:** 1–25

Vanroermund CWT, Elgersma Y, Singh N, Wanders RJA, Tabak HF (1995) The membrane of peroxisomes in Saccharomyces cerevisiae is impermeable to NAD(H) and acetyl-CoA under in vivo conditions. EMBO J **14:** 3480–3486

von Caemmerer S (2000) Biochemical Models of Leaf Photosynthesis. CSIRO Publishing, Collingwood, Australia

von Caemmerer S, Farquhar GD (1981) Some relationships between the biochemistry of photosynthesis and the gas exchange of leaves. Planta **153:** 376–387

Walton NJ, Butt VS (1981) Metabolism and decarboxylation of glycollate and serine in leaf peroxisomes. Planta **153:** 225–231

Wingler A, Lea P, Quick W, Leegood R (2000) Photorespiration: metabolic pathways and their role in stress protection. Philos Trans R Soc Lond B Biol Sci **355:** 1517–1529

Wingler A, Lea PJ, Leegood RC (1999) Photorespiratory metabolism of glyoxylate and formate in glycine-accumulating mutants of barley and Amaranthus edulis. Planta **207:** 518–526